

Vector Boson Fusion in the Inert Doublet Model

Bhaskar Dutta^{*}

Mitchell Institute for Fundamental Physics and Astronomy,

Department of Physics and Astronomy, Texas A&M University, College Station, TX 77843, USA

Guillermo Palacio[†], Diego Restrepo[‡]

Instituto de Física, Universidad de Antioquia, Calle 70 No. 52-21, Medellín, Colombia

José D. Ruiz-Álvarez[§]

Departamento de Física, Universidad de Los Andes, Código Postal 111711, Bogotá, Colombia

Month NN, YYYY

Abstract

In this paper we probe inert Higgs doublet model at the LHC using Vector Boson Fusion (VBF) search strategy. We optimize the selection cuts and investigate the parameter space of the model and we show that the VBF search has a better reach when compared with the monojet searches. We also investigate the Drell-Yan type cuts and show that they can be important for smaller charged Higgs masses. We determine the 3σ reach for the parameter space using these optimized cuts for a luminosity of 3000 fb^{-1} .

1 Introduction

The particle physics origin of the 27% of the universe is still unknown. The results from the direct, indirect detections and the collider experiment are investigating particle physics models which provide a dark matter candidate. The null results so far from these experiments have already ruled out many models. However, many models still exist with large regions of allowed parameter space. Since the LHC is ongoing, it will be crucial to come up with strategies to investigate the parameter spaces of these models to the maximum extent. In this paper, our main focus is to use the LHC searches to investigate one simple dark matter model by developing a search strategy and compare with the existing search strategies.

^{*}dutta@physics.tamu.edu

[†]galberto.palacio@udea.edu.co

[‡]restrepo@udea.edu.co

[§]jose.ruiz@cern.ch

One of the simplest models which provides a dark matter (DM) candidate is the Inert Doublet Model (IDM) [1, 2], where an additional scalar doublet of $SU(2)_L$ odd under a global Z_2 is added to the Standard Model (SM). The lightest neutral component of the scalar doublet acts as a dark matter candidate. Recent accounts of the model are given in [3–8], and further references are available therein. In particular, regarding the predictions of the model at colliders, the Drell-Yann (D-Y) production with lepton plus transverse missing energy signals at LHC have been extensively studied in the IDM as in [8–15]. We plan to investigate this model in this paper utilizing the Vector Boson Fusion (VBF) search strategy. Since the dark matter candidate of this model has weak charges, W , Z fusions are useful to produce these particles at the LHC. We will optimize the VBF cuts to improve the signal to the background ratio where the SM background mostly arises from $Z +$ jets. Utilizing the optimized cuts, we will show the reach of the LHC for the parameter space of the model in the ongoing and future runs. We will also compare this analysis with the existing search strategies.

We will investigate the LHC reach of the parameter space of the model without any restrictions arising from annihilation rate, direct and indirect detections since the correlations among these results to constrain the parameter space for the LHC requires many assumptions. For example, the annihilation rate constraint arising from the DM content requires a knowledge of the history of the universe prior to big bang nucleosynthesis (BBN) which is unconstrained. The origin of the dark matter content, e.g., may be due to thermal, non-thermal [16–22], non-standard cosmology (where the expansion rate can be different compared to the standard cosmology prior to the BBN) [23–27]. Consequently, the annihilation rate corresponding to the 27% can be very different compared to the thermal dark matter in standard cosmology and in some non-thermal scenarios, the dark matter content may not be related to any annihilation rate at all. We, therefore, plan to search for this model at the LHC without showing any preference for a particular cosmological scenario. Further, there can be multiple DM candidates (e.g., axion and DM from the inert doublet model) and in such scenarios [28, 29], the direct and indirect detection cross-sections should be reduced by R and R^2 respectively with $R \equiv \Omega h^2/0.12$. From all these considerations, it appears that the search at the LHC should be strategized without applying restrictions arising from the thermal annihilation rate and the direct and indirect detection constraints. If the signals from a particular physics model which possess a DM candidate are discovered at the LHC, we would not only be able to establish that model but it also would give us an opportunity to investigate the cosmology in the Pre-BBN era.

Following this strategy, the Monojet final state has been used effectively to search for parameter space of this model in ref. [4]. In this paper, we first optimize VBF cuts to search for the DM candidate in IDM. We will show that the VBF reach is better than the monojet final state. We will also show the parameter space where the D-Y type cuts can be important.

The paper is organized as follows. In section 2, we discuss the model. In section 3, we discuss the VBF signatures and develop VBF cuts. In section 4, we discuss the parameter space reach for this model at the LHC and we conclude in section 5.

2 The model

The Inert Doublet Model (IDM) is a minimal extension of the SM, where an additional $SU(2)_L$ scalar doublet, Φ , odd under a Z_2 discrete symmetry is added. The lightest neutral component of the scalar doublet is the dark matter candidate.

The Lagrangian of the model is given by:

$$\mathcal{L} = \mathcal{L}_{\text{SM}} + (D^\mu \Phi)^\dagger D_\mu \Phi - V(\Phi), \quad (1)$$

where

$$V(\Phi) = \mu_2^2 \Phi^\dagger \Phi + \lambda_2 (\Phi^\dagger \Phi)^2 + \lambda_3 (H^\dagger H)(\Phi^\dagger \Phi) + \lambda_4 (H^\dagger \Phi)(\Phi^\dagger H) + \frac{\lambda_5}{2} [(\Phi^\dagger H)^2 + \text{h.c.}] . \quad (2)$$

H stands for the Higgs doublet in the SM, which acquires a vacuum expectation value (VEV) $v = 246.2$ GeV. We define

$$\lambda_L = \frac{\lambda_3 + \lambda_4 + \lambda_5}{2} . \quad (3)$$

which controls the interactions through the Higgs portal. The components of the scalar doublets are defined as

$$\Phi = \begin{pmatrix} H^+ \\ \frac{1}{\sqrt{2}}(H^0 + iA^0) \end{pmatrix}, \quad H = \begin{pmatrix} G^+ \\ \frac{1}{\sqrt{2}}(v + h^0 + iG^0) \end{pmatrix} . \quad (4)$$

The fields are written in the canonical form. H^0 , A^0 and H^+ are the CP even, CP odd and charged scalar of the additional scalar doublet. G^+ and G^0 are the Goldstone bosons of the the $SU(2)_L \times U(1)_Y$ electroweak symmetry,

3 Search for VBF signature at the LHC

The IDM can be explored in the current and future runs of the large hadron collider (LHC) with a center of mass energy $\sqrt{s} = 13$ TeV. Since the DM candidate, H_0 has weak charges, it can be produced via a VBF strategy [30] at the LHC. The VBF search for the DM investigate missing energy in the association of two high E_T jet with large $|\Delta\eta|$ between the jets in the final state.

The important contributions to the VBF total cross-section for this model are displayed in figure 1. The last two diagrams are only important for large values of λ_L , while the first two diagrams can have large destructive interferences for small values of λ_L and not too large splitting between the set of inert scalar masses. The blob in the gluon diagram denotes the effective coupling between the gluons and the SM Higgs.

The inclusive cross section for the process $pp \rightarrow H^0 H^0 jj$ for a fixed dark matter mass of 150 GeV is displayed in figure 2 as a function of λ_L for several values of $M_{A^0} = M_{H^+}$. Note that for specific values of $M_{A^0} = M_{H^+}$, the Drell-Yann production of inert scalars for small λ_L can be enhanced, because of resonant production of gauge bosons which give rise to the two jets.

The VBF topology relies in a set of characteristic of the events from the point of view of a detector as the ATLAS or CMS experiments. The two jets produced from such signature are located in different hemispheres of the detector, which means that $\eta(j_1) \times \eta(j_2) < 0$. Additionally, these two jets are also well separated in the pseudorapidity. We expect then that the two jets from backgrounds faking the VBF topology have smaller separation in η than the two jets from our signal. Finally, a key characteristic of the two jets from the VBF topology is that their invariant mass is larger than

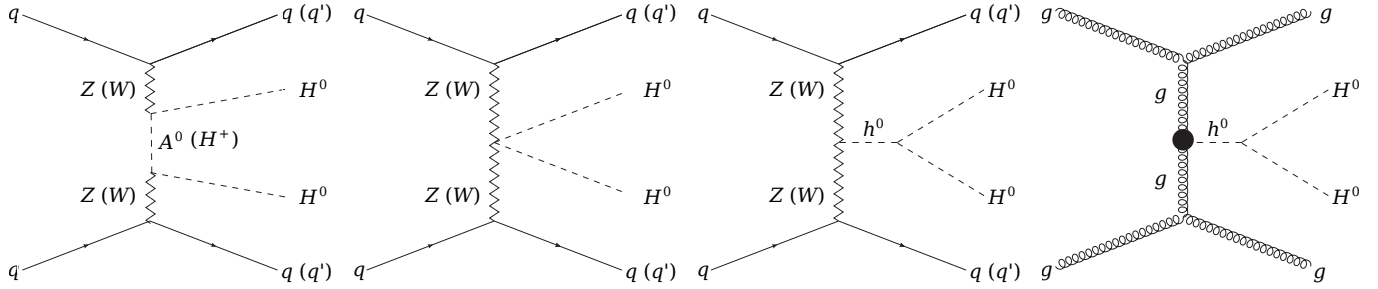


Figure 1: Feynman diagrams which contribute to $pp \rightarrow H^0 H^0 jj$ in the IDM

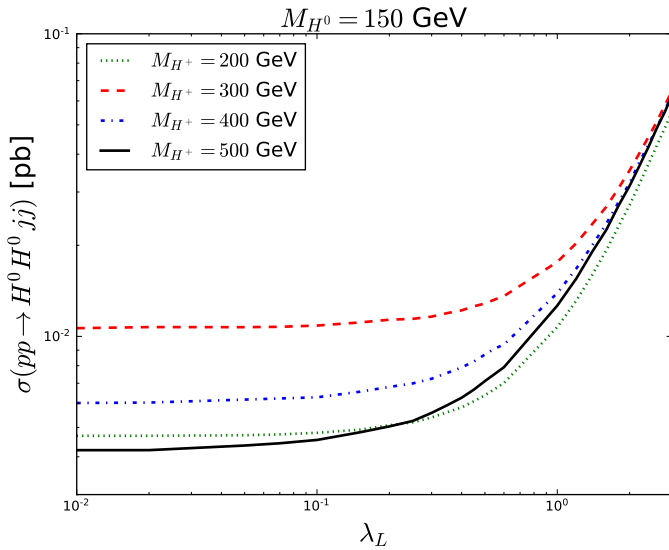


Figure 2: Cross section for the process $pp \rightarrow H^0 H^0 jj$ as a function of λ_L for $M_{H^0} = 150$ GeV, and several values of $M_{A^0} = M_{H^+}$.

for a couple of non-VBF jets. Some contributions to the VBF signal have been considered in [31] which does not include some of the essential VBF cuts, e.g., large $|\Delta\eta|$, large $M_{j_1 j_2}$ etc. Our cuts originate from the experimental searches as mentioned above [32, 33] which we optimize further. Consequently, we obtain much larger reach for the parameter space.

All these VBF characteristics significantly reduce backgrounds and gives us a different set of background than monojet searches. Our main backgrounds are $Z \rightarrow \nu\bar{\nu} + \text{jets}$ and $W^{+/-} \rightarrow l\bar{\nu} + \text{jets}$, where the lepton is missed by the detector reconstruction (for example if it is produced outside the experiment acceptance or fails isolation criteria). $Z \rightarrow \nu\bar{\nu} + \text{jets}$ background will be referred in the following as simply $Z + \text{jets}$. The QCD contribution to our background expectations is very small, and we consider it negligible for simplicity of this work.

To design our analysis we have used MC simulations of $Z + \text{jets}$ and the signal. We have used MadGraph [34] to simulate the partonic process while Pythia 8 [35] for the hadronization and showering. Finally, we have processed our samples with Delphes [36] to simulate a detector response. We have used default configurations from the packages and we have worked specifically with the CMS experiment simulation done by Delphes. We do not expect significant differences to our conclusions by switching the detector simulation to an ATLAS-like configuration. We have used AK4 (Anti- k_T

algorithm with $R = 0.4$) jets that are reconstructed with fastjet package [37]. Jets were reconstructed in a rapidity acceptance of $|\eta(j)| < 5$. For the simulation of the signal we have used the IDM model implementation [11, 38] available in the FeynRules [39] models database.

Based on the analysis presented in [32], we assume that the $W^{+-} + \text{jets}$ background is kinematically similar to the $Z + \text{jets}$ background. and that after full selection our background contribution will be composed 70% by Z -jets events and 30% by $W^{+-} + \text{jets}$. Moreover, as we just consider the significance

$$\sigma \equiv \frac{S}{\sqrt{S + B}}, \quad (5)$$

as figure of merit over the total number of events to determine the goodness of the selection, we are not affected by potential small kinematic differences between our two main backgrounds.

For the analysis we propose we relied in the following set of variables:

- $p_T^{\text{miss}} = -|\sum_{i=0}^{N(j)} \vec{p}_T(j_i)|$ denoted in the literature as transverse missing energy.
- $N(j)$ the jet multiplicity.
- The two leading jets p_T , $p_T(j_1)$ and $p_T(j_2)$.
- $\eta(j_1) \times \eta(j_2)$
- $|\Delta\eta(j_1, j_2)|$
- $M(j_1, j_2)$, the invariant mass of the two leading jets.

The selection was followed having the greatest significance in the order of the variables they have been cited. $N(j)$ was fixed to be greater than 1 and $\eta(j_1) \times \eta(j_2) < 0$. The signal samples used for the optimization was produced with $M_{H^0} = 65$ GeV, $M_{H^+} = M_{A^0} = 750$ GeV and $\lambda_L = 0.2$, but it has been checked that changing the λ_L parameter we do not gain re-optimizing the selection.

The set of cuts that drives the analysis to the greatest significance is:

Cut 1 : $p_T^{\text{miss}} > 180$ GeV

Cut 2 : $N(j) \geq 2$

Cut 3 : $p_T(j_1) > 100$ GeV

Cut 4 : $p_T(j_2) > 50$ GeV

Cut 5 : $\eta(j_1) \times \eta(j_2) < 0$

Cut 6 : $|\Delta\eta(j_1, j_2)| > 4.2$

Cut 7 : $M(j_1, j_2) > 1$ TeV

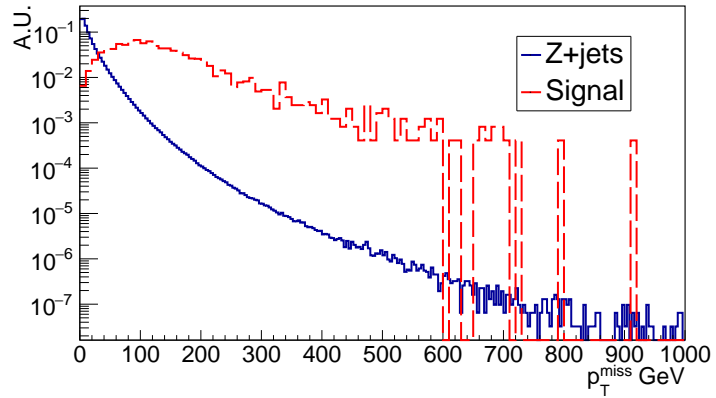


Figure 3: p_T^{miss} signal and $Z+\text{jets}$ background distributions before analysis selection. Both distributions have been normalized to unity.

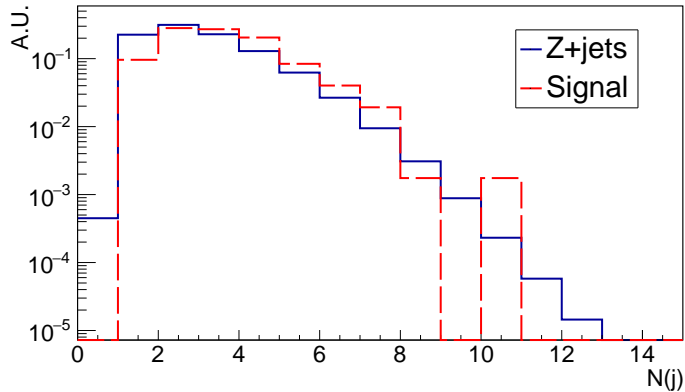


Figure 4: $N(j)$ signal and $Z+\text{jets}$ background distributions after cut 1. Both distributions have been normalized to unity.

The selection on the missing energy was chosen quite high because this variable is normally used for the trigger in the experiments for dark matter searches. It would be a good improvement for this search if this threshold could be lowered down as much as possible in the triggers used by the experiments. A comparison between signal and the main background on this variable before any cut can be found in figure 3. It can be seen that our signal is expected to have greater missing transverse momentum than the main background.

In figure 4 the jet multiplicity of our signal and main background after **Cut 1** is shown. Figure 5 shows the leading jets transverse momentum at the same stage of the selection and for the same samples. From the jets p_T distributions it can be seen that however the main background tends to have quite energetic first leading jet and a gain in sensitivity can be achieved cutting the events at the lower tail of the distribution. For the sub-leading jet, the signal shows clearly more energetic jets than the main background.

The pseudorapidity separation of the two leading jets is shown in figure 6 after **Cut 4**. We can corroborate from all these cited distributions that signal tends to have greatest separation between the two leading jets than the main background.

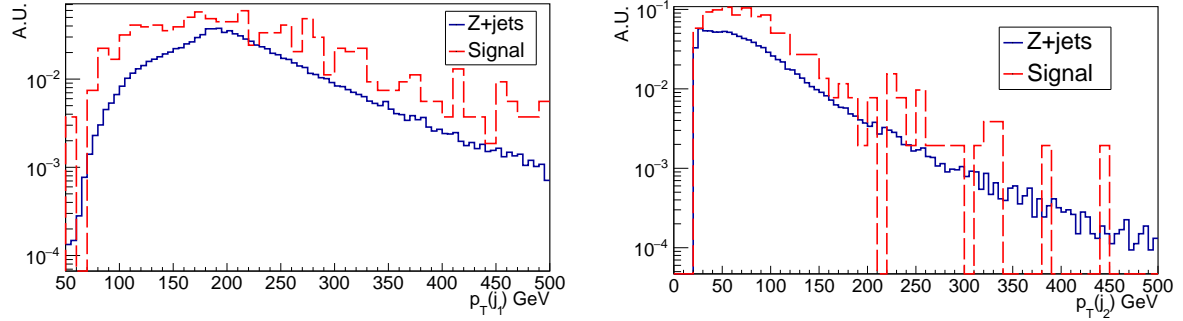


Figure 5: $p_T(j_1)$ (left) and $p_T(j_2)$ (right) signal and Z +jets background distributions before analysis selection. Both distributions have been normalized to unity.

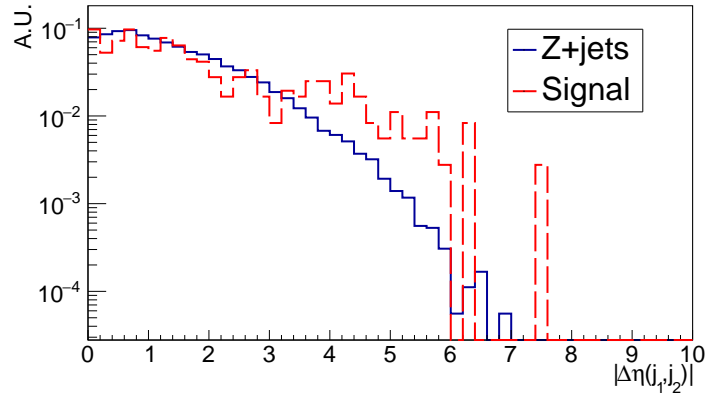


Figure 6: $\Delta\eta(j_1, j_2)$ signal and Z +jets background distributions after cut 4. Both distributions have been normalized to unity.

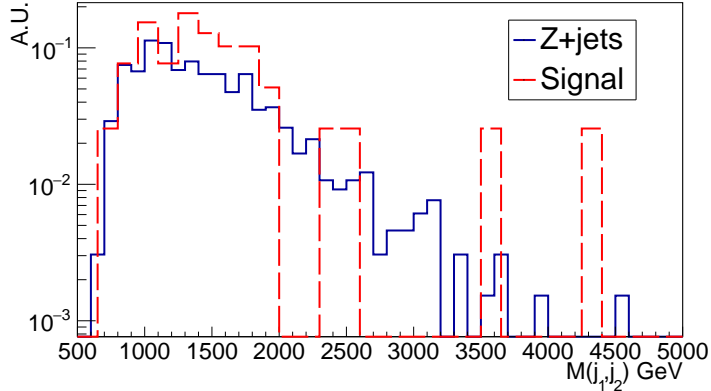


Figure 7: $M(j_1, j_2)$ signal and Z +jets background distributions after cut 6. Both distributions have been normalized to unity.

Finally, further differences between signal and the main background can be found in the invariant mass of the two leading jets. The distribution for signal and Z +jets background after cut 6 are shown in figure 7.

The efficiencies of each cut are displayed in table 1.

Process	Efficiency per cut		Cumulative efficiency	
	Signal	Z +jets	Signal	Z +jets
Initial number of MC events	2447	30996944	2447	30996944
Cut 1	$(23.38 \pm 0.86)\%$	$(0.22 \pm 8 \times 10^{-4})\%$	$(23.38 \pm 0.86)\%$	$(0.22 \pm 8 \times 10^{-4})\%$
Cut 4	$(63.11 \pm 2.02)\%$	$(51.95 \pm 0.19)\%$	$(14.75 \pm 0.72)\%$	$(0.12 \pm 6 \times 10^{-4})\%$
Cut 6	$(10.80 \pm 1.63)\%$	$(1.82 \pm 0.07)\%$	$(1.59 \pm 0.25)\%$	$(2.11 \times 10^{-3} \pm 8.3 \times 10^{-5})\%$
Cut 7	$(84.62 \pm 5.78)\%$	$(82.57 \pm 1.48)\%$	$(1.35 \pm 0.23)\%$	$(1.74 \times 10^{-3} \pm 7.5 \times 10^{-5})\%$

Table 1: Efficiencies for signal and Z +jets background for different stages of the selection.

In table 1 we have cited the efficiencies of the selection for a signal with $\lambda_L = 0.2$. These efficiencies actually have a dependence on this parameter. When λ_L is greater than 1, the first diagram displayed in figure 1 becomes subdominant, and therefore changing the selection efficiency. Therefore we have scanned λ_L between 0.01 and 10, and we found efficiencies between 1 and 5%. The efficiencies obtained from this scan have been used in the results section to calculate the significance as a function of λ_L . From table 1 we can see that Cut 7 is not resulting in a strong increase in the selection discrimination power. However, this cut, inspired from experimental results [32, 33], would be more discriminant with a different technique to estimate backgrounds as with data-driven methods.

4 Results

Using the cuts developed in table 1, we show the significances as a function of M_{H_0} in figures 8 and 9 for 30 and 3000 fb^{-1} luminosities and two different values of λ . In table 1 we have quoted only statistical uncertainties, however in our results we have considered a higher uncertainty of 30% over signal and background yields to have a more realistic approach including other sources of

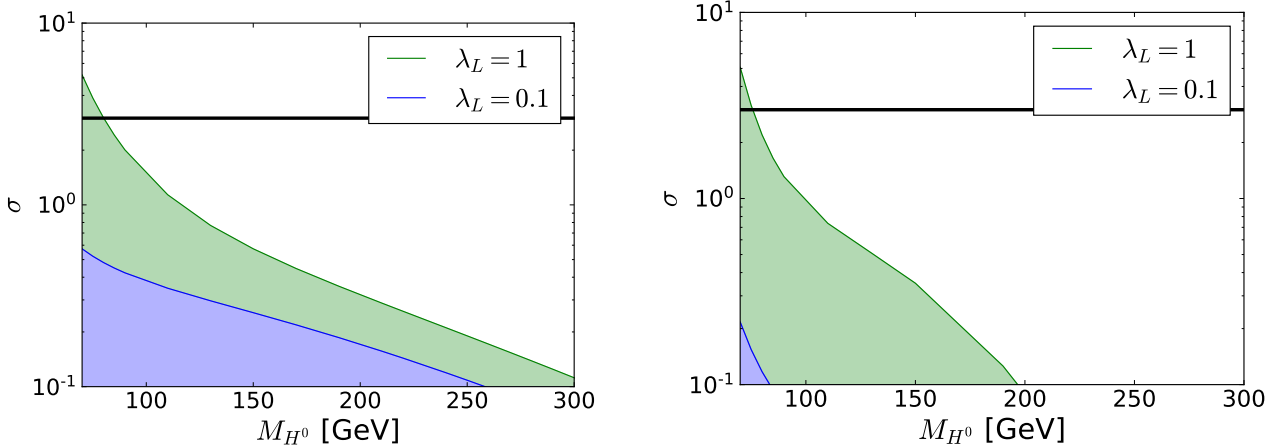


Figure 8: Significance for DM candidate discovery for a luminosity of 30 fb^{-1} . The charged scalar mass is 750 GeV (250 GeV) in the left (right) panel

λ_L	S_{MJ}	B_{MJ}	σ_{MJ}
0.01	3		0.015
0.1	3.7	134044	0.02
1.0	31		0.15

λ_L	S_{VBF}	B_{VBF}	σ_{VBF}
0.01	4.6		0.21
0.1	7.5	476	0.35
1.0	25		1.1

Table 2: Sensitivities for $M_{H^+} = M_{A^0} = 750 \text{ GeV}$ and $M_{H^0} = 110 \text{ GeV}$ for several λ_L values, with an integrated luminosity of 20 fb^{-1} .

uncertainties (e.g. PDF, cross section, ...). We find that larger values of M_{H^\pm} and λ_L produce larger significances for VBF analysis due to large production cross-sections. For $\lambda_L \sim 1$, the 3σ reach can go up to $M_{H^0} \sim 200 \text{ GeV}$ for 3000 fb^{-1} luminosity.

In figure 10, we show the 3σ reach of our VBF cuts in the λ_L and M_{H^0} parameter space for various luminosities ranging from 30 to 3000 fb^{-1} . We maximized the production cross-sections by choosing M_{H^\pm} appropriately. We can see that the reach for the parameter space is substantial. The 3σ reach of the parameter space of can go up to 280 GeV of M_{H^0} for larger values of λ_L . For $\lambda_L \sim 10^{-2}$, the 3σ reach for the DM mass goes up to $M_{H^0} \sim 125 \text{ GeV}$.

The IDM can be constrained using monojet-type searches at the LHC. However the reach of the VBF search is better than the monojet search. In Table 2, we compare the significances of monojet search using the cuts as given in [4, 40] with the VBF search strategy as developed in this paper at 20 fb^{-1} . In the table, S_{MJ} , S_{VBF} , B_{MJ} , B_{VBF} and $\sigma_{\text{MJ}, \text{VBF}}$ are signal, background events and significances for monojet and VBF selection cuts respectively where we find that the VBF searches are more effective in probing the IDM models.

If M_{H^+} is not so large ($< 500 \text{ GeV}$), H^+ can be produced efficiently with larger cross-section which then subsequently decay into H^0 . In such parameter space, Drell-Yan type cuts can be useful. In table 3, we show some Benchmark points where we vary H^+ , H^0 masses and λ_L to see effects on $\sigma(pp \rightarrow H^0 H^0 jj)$ where we find that if the charged Higgs mass is smaller, then the cross-section gets larger.

We then apply VBF and D-Y type cuts on all the scenarios where the D-Y type cuts are defined

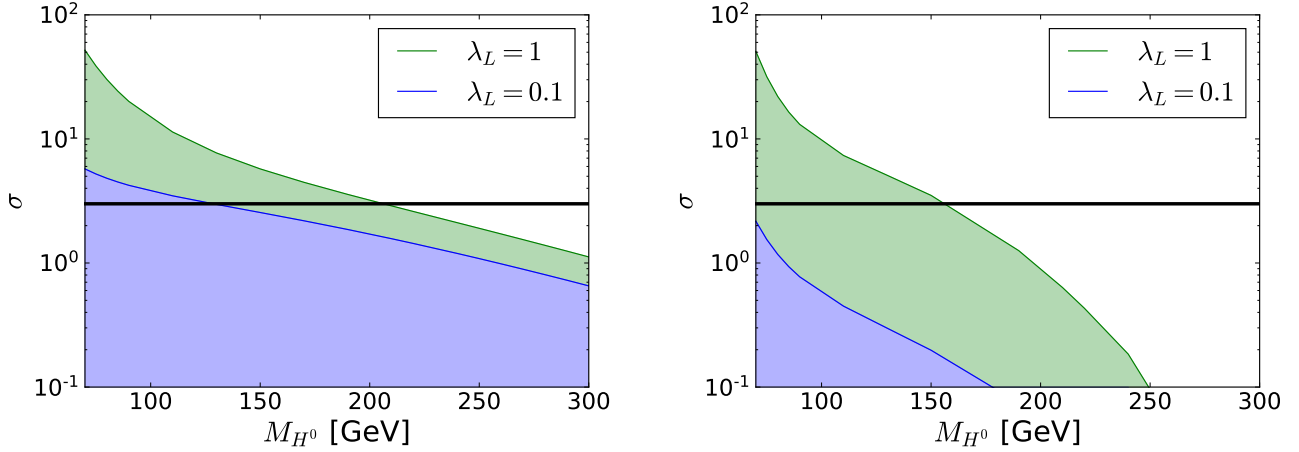


Figure 9: Significance for DM candidate discovery for a luminosity of 3000 fb^{-1} . The charged scalar mass is 750 GeV (250 GeV) in the left (right) panel

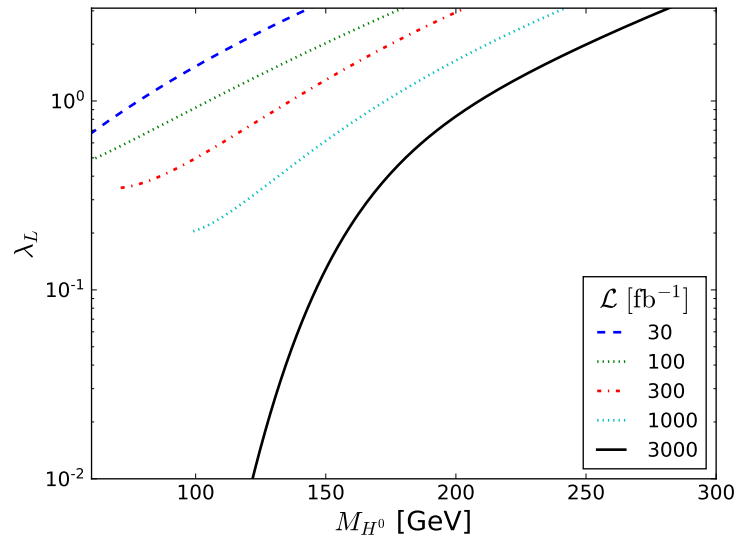


Figure 10: 3σ reach for λ_L vs M_{H^0} parameter space for various luminosities in fb^{-1} .

Benchmark	m_{H^+} [GeV]	m_{A^0} [GeV]	m_{H^0} [GeV]	λ_L	$\sigma(pp \rightarrow H^0 H^0 jj)$ [pb]
BP1	200	189.5	65	0.009	0.067
BP2	500	494	65	0.009	0.009
BP3	750	750	65	0.009	0.008
BP4	750	750	110	0.009	0.005
BP5	750	750	65	0.500	0.274

Table 3: Benchmark scenarios for the comparison

Benchmark	B_{DY}	S_{DY}	σ_{DY}	Benchmark	B_{VBF}	S_{VBF}	σ_{VBF}
BP1		148	1.59	BP1		38	0.25
BP2		68	0.73	BP2		198	1.28
BP3	8500	15	0.16	BP3	23809	309	1.99
BP4		10	0.11	BP4		234	1.51
BP5		85	0.92	BP5		3579	21.6

Table 4: Comparison between our analysis and the one implemented in Ref. [31], with an integrated luminosity of 1000 fb^{-1} .

in [31]: $N(j) = 2$, $N(b) = 0$, $N(l) = 0$, $p_T^{miss} > 260 \text{ GeV}$, $p_T(j_1) > 120 \text{ GeV}$, $p_T(j_2) > 90 \text{ GeV}$, $75 \text{ GeV} \leq M_{j_1 j_2} \leq 90 \text{ GeV}$, $\Delta R_{j_1 j_2} < 1.8$. We show our results in table 4 where we compare these cuts. In the table, $S_{\text{DY,VBF}}$, $B_{\text{DY,VBF}}$ and $\sigma_{\text{DY,VBF}}$ are signal, background events and significances for D-Y and VBF selection cuts respectively. We find that for $M_{H^+} \geq 500 \text{ GeV}$, the significance becomes much better for VBF analysis.

5 Conclusions

In this paper we utilize VBF search strategy to probe the parameter space of the inert doublet model where H_0 is a dark matter candidate. We probe the parameter space of the model at the LHC without applying constraints from the annihilation rate and the data from the direct and indirect experiments, since these constraints can be relaxed in various cosmological scenarios.

The VBF search is centered around the requirement of two high p_T jets which located in different hemispheres of the detector, $\eta(j_1) \times \eta(j_2) < 0$, which are also well separated in the pseudorapidity and their invariant mass is larger than for a couple of non-VBF jets. We further optimize the VBF cuts and found that $p_T^{miss} > 180 \text{ GeV}$, $p_T(j_{1(2)}) > 100(50) \text{ GeV}$, $|\Delta\eta| > 4.2$, $M(j_1, j_2) > 1 \text{ TeV}$, $N(j) \geq 2$, $\eta(j_1) \times \eta(j_2) < 0$ provide the largest significance. The dominant background arises from $Z + \text{jets}$ and we showed the signal and background distributions after each of these cuts. We showed that VBF search has a better reach when compared with the monojet searches. We also showed that for $M_{H^+} < 500 \text{ GeV}$, D-Y type of cuts provide better significances while VBF cut works much better for heavier M_{H^+} . We showed the 3σ reach of the $\lambda_L - M_{H^0}$ parameter space of the model using VBF cuts for various luminosities and found that the reach can go up to 280 GeV of Higgs mass for a luminosity of 3000 fb^{-1} .

6 Acknowledgments

B. D. acknowledges support from DOE Grant de-sc0010813. D. R. acknowledges support from the Grants Sostenibilidad-GFIF and CODI-IN650CE, and COLCIENCIAS through the Grant No. 111-565-84269. J. D. Ruiz-Álvarez gratefully acknowledges the support of COLCIENCIAS, the Administrative Department of Science, Technology and Innovation of Colombia.

References

- [1] Nilendra G. Deshpande and Ernest Ma, “Pattern of Symmetry Breaking with Two Higgs Doublets,” *Phys. Rev.* **D18**, 2574 (1978)
- [2] Riccardo Barbieri, Lawrence J. Hall, and Vyacheslav S. Rychkov, “Improved naturalness with a heavy Higgs: An Alternative road to LHC physics,” *Phys. Rev.* **D74**, 015007 (2006), [arXiv:hep-ph/0603188 \[hep-ph\]](https://arxiv.org/abs/hep-ph/0603188)
- [3] Benedikt Eiteneuer, Andreas Goudelis, and Jan Heisig, “The inert doublet model in the light of Fermi-LAT gamma-ray data: a global fit analysis,” *Eur. Phys. J.* **C77**, 624 (2017), [arXiv:1705.01458 \[hep-ph\]](https://arxiv.org/abs/1705.01458)
- [4] Alexander Belyaev, Giacomo Cacciapaglia, Igor P. Ivanov, Felipe Rojas, and Marc Thomas, “Anatomy of the Inert Two Higgs Doublet Model in the light of the LHC and non-LHC Dark Matter Searches,” (2016), [arXiv:1612.00511 \[hep-ph\]](https://arxiv.org/abs/1612.00511)
- [5] Federico von der Pahlen, Guillermo Palacio, Diego Restrepo, and Oscar Zapata, “Radiative Type III Seesaw Model and its collider phenomenology,” *Phys. Rev.* **D94**, 033005 (2016), [arXiv:1605.01129 \[hep-ph\]](https://arxiv.org/abs/1605.01129)
- [6] Camilo Garcia-Cely, Michael Gustafsson, and Alejandro Ibarra, “Probing the Inert Doublet Dark Matter Model with Cherenkov Telescopes,” *JCAP* **1602**, 043 (2016), [arXiv:1512.02801 \[hep-ph\]](https://arxiv.org/abs/1512.02801)
- [7] Farinaldo S. Queiroz and Carlos E. Yaguna, “The CTA aims at the Inert Doublet Model,” *JCAP* **1602**, 038 (2016), [arXiv:1511.05967 \[hep-ph\]](https://arxiv.org/abs/1511.05967)
- [8] Nikita Blinov, Jonathan Kozaczuk, David E. Morrissey, and Alejandro de la Puente, “Compressing the Inert Doublet Model,” *Phys. Rev.* **D93**, 035020 (2016), [arXiv:1510.08069 \[hep-ph\]](https://arxiv.org/abs/1510.08069)
- [9] Majid Hashemi and Saereh Najjari, “Observability of Inert Scalars at the LHC,” *Eur. Phys. J.* **C77**, 592 (2017), [arXiv:1611.07827 \[hep-ph\]](https://arxiv.org/abs/1611.07827)
- [10] Amitava Datta, Nabanita Ganguly, Najimuddin Khan, and Subhendu Rakshit, “Exploring collider signatures of the inert Higgs doublet model,” *Phys. Rev.* **D95**, 015017 (2017), [arXiv:1610.00648 \[hep-ph\]](https://arxiv.org/abs/1610.00648)
- [11] Genevieve Belanger, Beranger Dumont, Andreas Goudelis, Bjorn Herrmann, Sabine Kraml, and Dipan Sengupta, “Dilepton constraints in the Inert Doublet Model from Run 1 of the LHC,” *Phys. Rev.* **D91**, 115011 (2015), [arXiv:1503.07367 \[hep-ph\]](https://arxiv.org/abs/1503.07367)

- [12] Michael Gustafsson, Sara Rydbeck, Laura Lopez-Honorez, and Erik Lundstrom, “Status of the Inert Doublet Model and the Role of multileptons at the LHC,” *Phys. Rev.* **D86**, 075019 (2012), [arXiv:1206.6316 \[hep-ph\]](https://arxiv.org/abs/1206.6316)
- [13] Xinyu Miao, Shufang Su, and Brooks Thomas, “Trilepton Signals in the Inert Doublet Model,” *Phys. Rev.* **D82**, 035009 (2010), [arXiv:1005.0090 \[hep-ph\]](https://arxiv.org/abs/1005.0090)
- [14] Ethan Dolle, Xinyu Miao, Shufang Su, and Brooks Thomas, “Dilepton Signals in the Inert Doublet Model,” *Phys. Rev.* **D81**, 035003 (2010), [arXiv:0909.3094 \[hep-ph\]](https://arxiv.org/abs/0909.3094)
- [15] Qing-Hong Cao, Ernest Ma, and G. Rajasekaran, “Observing the Dark Scalar Doublet and its Impact on the Standard-Model Higgs Boson at Colliders,” *Phys. Rev.* **D76**, 095011 (2007), [arXiv:0708.2939 \[hep-ph\]](https://arxiv.org/abs/0708.2939)
- [16] John D. Barrow, “Massive particles as a probe of the early universe,” *Nucl. Phys.* **B208**, 501–508 (1982)
- [17] Marc Kamionkowski and Michael S. Turner, “Thermal relics: do we know their abundances?,” *Phys. Rev.* **D42**, 3310–3320 (1990)
- [18] Takeo Moroi and Lisa Randall, “Wino cold dark matter from anomaly mediated SUSY breaking,” *Nucl. Phys.* **B570**, 455–472 (2000), [arXiv:hep-ph/9906527 \[hep-ph\]](https://arxiv.org/abs/hep-ph/9906527)
- [19] Masaaki Fujii and Koichi Hamaguchi, “Higgsino and wino dark matter from Q ball decay,” *Phys. Lett.* **B525**, 143–149 (2002), [arXiv:hep-ph/0110072 \[hep-ph\]](https://arxiv.org/abs/hep-ph/0110072)
- [20] Graciela B. Gelmini and Paolo Gondolo, “Neutralino with the right cold dark matter abundance in (almost) any supersymmetric model,” *Phys. Rev.* **D74**, 023510 (2006), [arXiv:hep-ph/0602230 \[hep-ph\]](https://arxiv.org/abs/hep-ph/0602230)
- [21] Ryuichiro Kitano, Hitoshi Murayama, and Michael Ratz, “Unified origin of baryons and dark matter,” *Phys. Lett.* **B669**, 145–149 (2008), [arXiv:0807.4313 \[hep-ph\]](https://arxiv.org/abs/0807.4313)
- [22] Bhaskar Dutta, Louis Leblond, and Kuver Sinha, “Mirage in the Sky: Non-thermal Dark Matter, Gravitino Problem, and Cosmic Ray Anomalies,” *Phys. Rev.* **D80**, 035014 (2009), [arXiv:0904.3773 \[hep-ph\]](https://arxiv.org/abs/0904.3773)
- [23] Riccardo Catena, N. Fornengo, A. Masiero, Massimo Pietroni, and Francesca Rosati, “Dark matter relic abundance and scalar - tensor dark energy,” *Phys. Rev.* **D70**, 063519 (2004), [arXiv:astro-ph/0403614 \[astro-ph\]](https://arxiv.org/abs/astro-ph/0403614)
- [24] Graciela B. Gelmini and Paolo Gondolo, “Ultra-cold WIMPs: relics of non-standard pre-BBN cosmologies,” *JCAP* **0810**, 002 (2008), [arXiv:0803.2349 \[astro-ph\]](https://arxiv.org/abs/0803.2349)
- [25] A. B. Lahanas, N. E. Mavromatos, and Dimitri V. Nanopoulos, “Dilaton and off-shell (non-critical string) effects in Boltzmann equation for species abundances,” *PMC Phys.* **A1**, 2 (2007), [arXiv:hep-ph/0608153 \[hep-ph\]](https://arxiv.org/abs/hep-ph/0608153)
- [26] Michael T. Meehan and Ian B. Whittingham, “Dark matter relic density in scalar-tensor gravity revisited,” *JCAP* **1512**, 011 (2015), [arXiv:1508.05174 \[astro-ph.CO\]](https://arxiv.org/abs/1508.05174)

[27] Bhaskar Dutta, Esteban Jimenez, and Ivonne Zavala, “Dark Matter Relics and the Expansion Rate in Scalar-Tensor Theories,” *JCAP* **1706**, 032 (2017), [arXiv:1612.05553 \[hep-ph\]](https://arxiv.org/abs/1612.05553)

[28] Howard Baer, Vernon Barger, Peisi Huang, Dan Mickelson, Maren Padelfke-Kirkland, and Xerxes Tata, “Natural SUSY with a bino- or wino-like LSP,” *Phys. Rev.* **D91**, 075005 (2015), [arXiv:1501.06357 \[hep-ph\]](https://arxiv.org/abs/1501.06357)

[29] Luis Aparicio, Michele Cicoli, Bhaskar Dutta, Sven Krippendorf, Anshuman Maharana, Francesco Muia, and Fernando Quevedo, “Non-thermal CMSSM with a 125 GeV Higgs,” *JHEP* **05**, 098 (2015), [arXiv:1502.05672 \[hep-ph\]](https://arxiv.org/abs/1502.05672)

[30] Andres G. Delannoy *et al.*, “Probing Dark Matter at the LHC using Vector Boson Fusion Processes,” *Phys. Rev. Lett.* **111**, 061801 (2013), [arXiv:1304.7779 \[hep-ph\]](https://arxiv.org/abs/1304.7779)

[31] P. Poulose, Shibananda Sahoo, and K. Sridhar, “Exploring the Inert Doublet Model through the dijet plus missing transverse energy channel at the LHC,” *Phys. Lett.* **B765**, 300–306 (2017), [arXiv:1604.03045 \[hep-ph\]](https://arxiv.org/abs/1604.03045)

[32] Vardan Khachatryan *et al.* (CMS), “Search for Dark Matter and Supersymmetry with a Compressed Mass Spectrum in the Vector Boson Fusion Topology in Proton-Proton Collisions at $\sqrt{s} = 8$ TeV,” *Phys. Rev. Lett.* **118**, 021802 (2017), [arXiv:1605.09305 \[hep-ex\]](https://arxiv.org/abs/1605.09305)

[33] Georges Aad *et al.* (ATLAS), “Search for invisible decays of a Higgs boson using vector-boson fusion in pp collisions at $\sqrt{s} = 8$ TeV with the ATLAS detector,” *JHEP* **01**, 172 (2016), [arXiv:1508.07869 \[hep-ex\]](https://arxiv.org/abs/1508.07869)

[34] J. Alwall, R. Frederix, S. Frixione, V. Hirschi, F. Maltoni, O. Mattelaer, H. S. Shao, T. Stelzer, P. Torrielli, and M. Zaro, “The automated computation of tree-level and next-to-leading order differential cross sections, and their matching to parton shower simulations,” *JHEP* **07**, 079 (2014), [arXiv:1405.0301 \[hep-ph\]](https://arxiv.org/abs/1405.0301)

[35] Torbjörn Sjöstrand, Stefan Ask, Jesper R. Christiansen, Richard Corke, Nishita Desai, Philip Ilten, Stephen Mrenna, Stefan Prestel, Christine O. Rasmussen, and Peter Z. Skands, “An Introduction to PYTHIA 8.2,” *Comput. Phys. Commun.* **191**, 159–177 (2015), [arXiv:1410.3012 \[hep-ph\]](https://arxiv.org/abs/1410.3012)

[36] J. de Favereau, C. Delaere, P. Demin, A. Giannanco, V. Lemaître, A. Mertens, and M. Selvaggi (DELPHES 3), “DELPHES 3, A modular framework for fast simulation of a generic collider experiment,” *JHEP* **02**, 057 (2014), [arXiv:1307.6346 \[hep-ex\]](https://arxiv.org/abs/1307.6346)

[37] Matteo Cacciari, Gavin P. Salam, and Gregory Soyez, “FastJet User Manual,” *Eur. Phys. J.* **C72**, 1896 (2012), [arXiv:1111.6097 \[hep-ph\]](https://arxiv.org/abs/1111.6097)

[38] A. Goudelis, B. Herrmann, and O. Stål, “Dark matter in the Inert Doublet Model after the discovery of a Higgs-like boson at the LHC,” *JHEP* **09**, 106 (2013), [arXiv:1303.3010 \[hep-ph\]](https://arxiv.org/abs/1303.3010)

[39] Adam Alloul, Neil D. Christensen, Céline Degrande, Claude Duhr, and Benjamin Fuks, “FeynRules 2.0 - A complete toolbox for tree-level phenomenology,” *Comput. Phys. Commun.* **185**, 2250–2300 (2014), [arXiv:1310.1921 \[hep-ph\]](https://arxiv.org/abs/1310.1921)

[40] Morad Aaboud *et al.* (ATLAS), “Search for new phenomena in final states with an energetic jet and large missing transverse momentum in pp collisions at 13 TeV using the ATLAS detector,” *Phys. Rev.* **D94**, 032005 (2016), [arXiv:1604.07773 \[hep-ex\]](https://arxiv.org/abs/1604.07773)